

Half-Marker Codes for Deletion Channels with Applications in DNA Storage

Javad Haghghat and Tolga M. Duman, *Fellow, IEEE*

Abstract—DNA data storage systems face significant challenges, including insertion, deletion, and substitution (IDS) errors. Therefore, designing effective synchronization codes, i.e., codes capable of correcting IDS errors, is essential for DNA storage systems. Marker codes are a favorable choice for this purpose. In this paper, we extend the notion of marker codes by making the following key observation. Since each DNA base is equivalent to a 2-bit storage unit, one bit can be reserved for synchronization, while the other is dedicated to data transmission. Using this observation, we propose a new class of marker codes, which we refer to as half-marker codes. We demonstrate that this extension has the potential to significantly increase the mutual information between the input sequence and the soft outputs of an IDS channel modeling a DNA storage system. Specifically, through examples, we show that when concatenated with an outer error-correcting code, half-marker codes outperform standard marker codes and significantly reduce the end-to-end bit error rate of the system.

Index Terms—Marker codes, insertion and deletion channels, DNA storage systems.

I. INTRODUCTION

DNA data storage systems offer a tremendous increase in recording densities, as well as significantly longer lifetimes compared to conventional storage systems [1],[2]. The cost of DNA storage systems has constantly reduced throughout the last decade, thanks to the invention of cost-efficient DNA synthesis (writing) and DNA sequencing (reading) techniques, including the nanopore sequencing method [3]. However, such cost-efficient techniques amplify the presence of insertion, deletion, and substitution (IDS) errors [1]-[4]. Unlike substitution errors, which only alter one base, an insertion or deletion error shifts all subsequent bases and can potentially corrupt large portions of data. Hence, even a few insertion and deletion errors in a transmitted block can render standard error-correcting codes ineffective. Therefore, the synthesized data must be protected by codes designed to correct insertion and deletion errors, also known as synchronization errors. The design of efficient coding and decoding schemes for transmission over channels with synchronization errors has been considered in several recent

works including [5]-[12] and the references therein, among others.

Marker codes, originally introduced in [13], are a class of synchronization error-correcting codes, which are broadly employed in DNA storage systems [14], [15], [16] due to their simple structure and efficient decoding algorithms. In standard marker coding, the values of certain transmitted symbols referred to as marker symbols, which are located at specified positions of the transmitted sequence, are fixed, and known at the decoder. The decoder exploits this *a priori* information, i.e., positions and values of the marker symbols, to correct the synchronization errors by employing a forward-backward (FB) decoding algorithm [17].

In this paper, we introduce a new class of marker codes for DNA storage systems, referred to as half-marker codes. A half-marker symbol is defined as a symbol of a 4-ary alphabet in which one bit has a fixed value and contributes to maintaining synchronization, whereas the second bit is an information-carrying bit that may take 0 or 1 with equal probabilities (depending on the information bit embedded in this symbol). Therefore, unlike standard marker symbols that are designed solely for synchronization purposes, half-markers are synchronization symbols that are also capable of carrying one bit of information. We show that for a digital communication system that models a DNA storage system, the mutual information between the input symbols and their corresponding soft outputs may significantly increase when standard marker codes are replaced by the proposed half-marker codes. In addition to mutual information estimation, we also provide explicit concatenated coding schemes when a low-density parity check (LDPC) code is applied as the outer code, and the marker code is employed as the inner code. Our numerical results show that the specific half-marker codes have the potential to significantly reduce the end-to-end bit error rate compared to standard marker codes in concatenated coding schemes.

The system model and preliminary definitions are given in Section II. In Section III, we present the proposed half-marker codes and discuss approaches to evaluate their efficiency. In Section IV, performance of the proposed half-marker codes is compared with the performance of the standard markers via numerical examples. Section V concludes this paper.

II. SYSTEM MODEL

The considered system model is shown in Fig. 1. An n -bit information sequence, \mathbf{u} , is converted to a 4-ary vector \mathbf{s} of length $\frac{n}{2}$ (assuming n is even). We denote the 4-ary

J. Haghghat is with the Department of Electrical and Electronics Engineering, TED University, 06420 Ankara, Turkey. T. M. Duman is with the Department of Electrical and Electronics Engineering, Bilkent University, 06800 Ankara, Turkey (e-mail: javad.haghghat@tedu.edu.tr, duman@ee.bilkent.edu.tr)

This work was funded by the European Union through the ERC Advanced Grant 101054904: TRANCIDS. Views and opinions expressed are, however, those of the authors only and do not necessarily reflect those of the European Union or the European Research Council Executive Agency. Neither the European Union nor the granting authority can be held responsible for them.

alphabet by $\{00, 01, 10, 11\}$ and the i -th symbol of \mathbf{s} by $s_i \in \{00, 01, 10, 11\}$. The binary to 4-ary mapping is defined as $s_i = u_{2i-1}u_{2i}$, where $u_j \in \{0, 1\}$ denotes the j -th bit of \mathbf{u} . The marker coding process combines known symbols, referred to as marker symbols, with \mathbf{s} , in order to protect the data against synchronization errors. This concatenation leads to a 4-ary codeword, \mathbf{x} . The rate of the marker code, denoted as r_M , is determined by dividing the length of \mathbf{s} by the length of \mathbf{x} .

The codeword, \mathbf{x} , is synthesized into a DNA strand, by employing a one-to-one mapping between the 4-ary alphabet symbols and the four DNA bases. The DNA strands are then stored in a DNA storage unit. Accessing the stored data is realized through a DNA sequencing process which converts the DNA strand back into a 4-ary vector, \mathbf{y} . However, the sequencing process is imperfect due to the occurrence of insertion, deletion, and substitution errors. In this work, we primarily focus on deletion and substitution errors, although insertion errors are also included in our numerical results. More precisely, we model the end-to-end communication channel between \mathbf{x} and \mathbf{y} as a deletion/substitution channel, as follows. (i) The i -th symbol of \mathbf{x} , denoted by x_i , is either deleted with a probability p_d or is transmitted with a probability $1 - p_d$, where a deletion event is defined as the event that no output symbol is generated corresponding to the channel input, x_i . (ii) If x_i is not deleted, it is either correctly received, with probability $1 - p_s$, or is substituted by a symbol $y_j \neq x_i$, where y_j is a realization of a random variable which is uniformly distributed over the set $\{00, 01, 10, 11\} \setminus \{x_i\}$. The deletion/substitution events are independent across the entire sequence. Channel parameters p_d and p_s are referred to as the deletion probability and the substitution probability, respectively.

The received vector, \mathbf{y} , is delivered to an FB decoder that generates four real-valued (soft) output vectors $\boldsymbol{\rho}^{00}, \boldsymbol{\rho}^{01}, \boldsymbol{\rho}^{10}, \boldsymbol{\rho}^{11}$. The i -th entries of these vectors, denoted by $\rho_i^{00}, \dots, \rho_i^{11}$, are the *a posteriori* probabilities calculated by the FB decoder, i.e.,

$$\begin{bmatrix} \rho_i^{00} \\ \rho_i^{01} \\ \rho_i^{10} \\ \rho_i^{11} \end{bmatrix} = \begin{bmatrix} Pr(s_i = 00|\mathbf{y}) \\ Pr(s_i = 01|\mathbf{y}) \\ Pr(s_i = 10|\mathbf{y}) \\ Pr(s_i = 11|\mathbf{y}) \end{bmatrix} \quad (1)$$

Finally, a vector of log-likelihood ratios (LLRs), $\mathbf{L} = (L_1, \dots, L_n)$, corresponding to the binary information sequence, \mathbf{u} , is derived by using

$$L_j = \log \frac{Pr(u_j = 1|\mathbf{y})}{Pr(u_j = 0|\mathbf{y})} \quad (2)$$

for $j \in \{1, \dots, n\}$. By recalling the 4-ary mapping $s_i = u_{2i-1}u_{2i}$ and using (1), it is straightforward to show that:

$$\begin{aligned} Pr(u_{2i-1} = 1|\mathbf{y}) &= \rho_i^{10} + \rho_i^{11} \\ Pr(u_{2i-1} = 0|\mathbf{y}) &= \rho_i^{00} + \rho_i^{01} \\ Pr(u_{2i} = 1|\mathbf{y}) &= \rho_i^{01} + \rho_i^{11} \\ Pr(u_{2i} = 0|\mathbf{y}) &= \rho_i^{00} + \rho_i^{10} \end{aligned} \quad (3)$$

for $i \in \{1, \dots, \frac{n}{2}\}$. Hence, L_j is found by plugging (3) into (2). It is worth noting that in most practical schemes, the marker

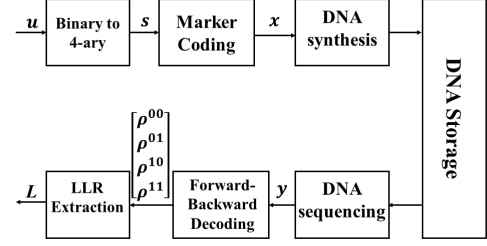


Figure 1. Block diagram of the considered DNA storage system.

code is concatenated with an outer error-correcting code, in which case vector \mathbf{u} of Fig. 1 is a codeword of the outer code. The LLR vector \mathbf{L} is delivered to the outer code's decoder, which updates the LLR values and feeds them back to the inner decoder for subsequent iterations. An estimate of \mathbf{u} is generated after a specified number of LLR exchanges between the inner and the outer decoders.

III. HALF-MARKER CODES

In this section, we propose half-marker codes as an alternative to standard marker codes. We define a half-marker symbol as a symbol in one of the forms: $1x, 0x, x1$, or $x0$, where x denotes an information bit which could be either 0 or 1, with equal probability. For example, a $1x$ half-marker symbol is defined as a symbol that takes on the values 10 or 11, each with probability 0.5. Using this definition, corresponding to each standard marker code which periodically inserts N_m markers, we will define a half-marker code that periodically inserts $2N_m$ half-markers.

To formally define the proposed half-marker codes, let us first give a formal definition for standard marker codes. Let $\mathbf{m} = (b_1b'_1, \dots, b_{N_m}b'_{N_m})$ be a 4-ary vector of length N_m (i.e., $b_i \in \{0, 1\}$ and $b'_i \in \{0, 1\}$). Let $N_p > N_m$ be an integer, and define $N_d = N_p - N_m$. Define an (N_p, \mathbf{m}) standard marker code as a code that encodes an input vector $\mathbf{s} = (s_1, \dots, s_{\frac{n}{2}})$ into a codeword \mathbf{x} such that:

$$\begin{cases} \mathbf{x}_{kN_p+1}^{(k+1)N_p} = (\mathbf{m}, \mathbf{s}_{kN_d+1}^{(k+1)N_d}), & k \in \{0, \dots, K-1\} \\ \mathbf{x}_{KN_p+1}^{KN_p+N_m+r} = (\mathbf{m}, \mathbf{s}_{KN_d+1}^{KN_d+r}), & r \neq 0 \end{cases} \quad (4)$$

where $\frac{n}{2} = KN_d + r$ for integers $K \geq 0$ and $0 \leq r \leq N_d - 1$; $\mathbf{x}_{kN_p+1}^{(k+1)N_p}$ denotes the vector $(x_{kN_p+1}, \dots, x_{(k+1)N_p})$, and $(\mathbf{m}, \mathbf{s}_{kN_d+1}^{(k+1)N_d})$ denotes concatenation of vectors \mathbf{m} and $\mathbf{s}_{kN_d+1}^{(k+1)N_d}$. In words, the codeword \mathbf{x} expressed in (4) is generated by taking the following steps. First, the encoder calculates that for transmitting all $\frac{n}{2}$ symbols of \mathbf{s} , K segments of length N_d and one extra segment of length r is required, where $r \neq 0$ if and only if N_d does not divide $\frac{n}{2}$. Then, the encoder periodically inserts the N_m marker symbols, specified by the vector \mathbf{m} , before each length- N_d segment of the data vector \mathbf{s} . Finally, if

$r \neq 0$, the encoder appends one last segment consisting of the marker symbols followed by the r remaining symbols of \mathbf{s} .

Now, let us define a vector of $2N_m$ half-marker symbols with marker bits corresponding to $\mathbf{m} = (b_1 b'_1, \dots, b_{N_m} b'_{N_m})$, and information bits corresponding to $\mathbf{u}_{2i+1}^{2i+2N_m}$, as follows:

$$\mathbf{h}_{2i+1}^{2i+2N_m} = \left(b_1 u_{2i+1}, b'_1 u_{2i+2}, \dots, b_{N_m} u_{2N_m+1}, b'_{N_m} u_{2N_m+2} \right) \quad (5)$$

From the mapping $s_j = u_{2j-1} u_{2j}$, it is clear that the N_m information symbols, $\mathbf{s}_{i+1}^{i+N_m}$, are embedded in the $2N_m$ half-marker symbols, $\mathbf{h}_{2i+1}^{2i+2N_m}$. We define an (N_p, \mathbf{m}) half-marker code, for $N_p \geq 2N_m$, as a code that generates a codeword \mathbf{x} as follows:

$$\begin{cases} \mathbf{x}_{kN_p+1}^{(k+1)N_p} = \left(\mathbf{h}_{2kN_d+1}^{2kN_d+2N_m}, \mathbf{s}_{kN_d+N_m+1}^{(k+1)N_d} \right), & 0 \leq k < K \\ \mathbf{x}_{KN_p+r}^{KN_p+r} = \mathbf{h}_{2KN_d+1}^{2KN_d+2r}, & 0 < r \leq 2N_m \\ \mathbf{x}_{KN_p+r}^{KN_p+r} = \left(\mathbf{h}_{2KN_d+1}^{2KN_d+2N_m}, \mathbf{s}_{KN_d+N_m+1}^{KN_d+r} \right), & r > 2N_m \end{cases} \quad (6)$$

The first row in (6) states that the half-marker code periodically inserts $2N_m$ half-marker symbols before each block of $N_d - N_m$ information symbols. Since N_m information symbols, $\mathbf{s}_{kN_d+1}^{kN_d+N_m}$, are embedded into the $2N_m$ half-marker symbols, $\mathbf{h}_{2kN_d+1}^{2kN_d+2N_m}$, each N_p symbols of the codeword \mathbf{x} include a total of N_d information symbols. Therefore, the rate of the proposed (N_p, \mathbf{m}) half-marker code is equal to the rate of the (N_p, \mathbf{m}) standard marker code.

Figure 2 illustrates and compares the placement of standard markers and half-markers within a data sequence. To intuitively explain the potential advantage of half-marker codes, note that a 4-ary transmission can be interpreted as simultaneous transmission of two parallel binary sequences (as also depicted in Fig. 2). Since insertions and deletions introduced by the IDS channel affect both binary sequences at the same positions, restoring synchronization in just one of them is theoretically sufficient. Therefore, a logical strategy is to allocate more markers to one sequence to enhance its resilience against insertion-deletion noise while omitting markers from the other—effectively implementing half-markers.

Note that in order to properly decode half-marker codes, the FB decoding algorithm must be modified to account for the changed statistics of the transmitted codeword, \mathbf{x} . A detailed version of the FB decoding equations is presented in [20], where the effect of this modification is reflected in the definition of the alignment function, ζ , defined as follows:

$$\zeta(j, a) = \sum_{a' \in \{00, \dots, 11\}} P(x_j = a') \times f(a', a), \quad (7)$$

where $f(a', a) = 1 - p_s$ for $a = a'$ and $f(a', a) = \frac{p_s}{3}$ for $a \neq a'$. When a half-marker symbol is placed at the j -th position, the symbol x_j becomes a random variable that takes two possible values with equal probabilities, i.e., $P(x_j = a') = 0.5$ for two values of a' . This differs from the case of a standard marker symbol, where $P(x_j = a') = 1$ when a' is equal to the

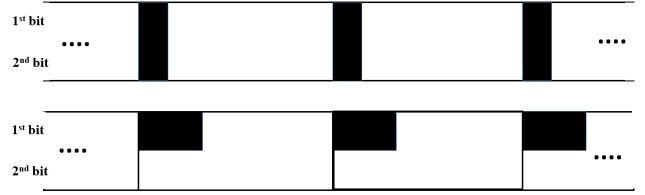


Figure 2. Comparison between inserting standard markers (Top) and half-markers (Bottom) within a 4-ary data sequence. Marker bits are shown in black, and data bits are shown in white.

marker symbol, and is zero otherwise. Function ζ defined above is further employed to calculate the forward and backward coefficients, referred to as α and β (see [20]-Equations (15) and (16)).

To compare the theoretical performance limits of (N_p, \mathbf{m}) standard and half-marker codes, we employ the *overall achievable rate* as the theoretical performance metric. Consider the concatenation of a binary outer code with the marker code, such that the binary sequence \mathbf{u} shown in Fig. 1 is a codeword generated by that binary outer code, and the LLR vector, \mathbf{L} , is delivered to a decoder of that binary outer code to obtain an estimate of \mathbf{u} . Let $I(\mathbf{u}; \mathbf{L})$ denote the mutual information between \mathbf{u} and its corresponding LLR vector, \mathbf{L} . Then, $\frac{1}{n} I(\mathbf{u}; \mathbf{L})$ is an achievable rate for the above-mentioned binary outer code. Hence, the following overall rate is achievable when a marker code with rate r_M is concatenated with a binary outer code:

$$R_a = \frac{r_M}{n} \times I(\mathbf{u}; \mathbf{L}). \quad (8)$$

To estimate $I(\mathbf{u}; \mathbf{L})$, we adopt the approach proposed in [18], as explained in the following (note that, with a slight abuse of notation, random variables and their realizations are represented using the same symbol). Assuming that u_j 's are unbiased, independent, and identically distributed, we approximate $I(\mathbf{u}; \mathbf{L}) \approx \sum_{j=1}^n I(u_j; L_j)$, where

$$I(u_j; L_j) = H(L_j) - H(L_j|u_j), \quad (9)$$

and $H(\cdot)$ denotes entropy. Notably,

$$H(L_j|u_j) = \frac{1}{2}H(L_j|u_j = 0) + \frac{1}{2}H(L_j|u_j = 1). \quad (10)$$

To estimate $H(L_j)$, $H(L_j|u_j = 0)$, and $H(L_j|u_j = 1)$, we approximate their empirical distributions via simulation. Specifically, we choose a large n (e.g., 10^4), randomly generate u_j 's, simulate a realization of the channel, perform forward-backward decoding, and compute L_j 's. We then define two sets, \mathcal{A}_0 and \mathcal{A}_1 , and update them as follows. If $u_j = 0$, we append L_j to \mathcal{A}_0 ; otherwise, we append L_j to \mathcal{A}_1 . This process is repeated multiple times (e.g., 10000 iterations). Finally, the recorded values in \mathcal{A}_0 , \mathcal{A}_1 , and $\mathcal{A}_0 \cup \mathcal{A}_1$ are used to approximate $H(L_j|u_j = 0)$, $H(L_j|u_j = 1)$, and $H(L_j)$, respectively, using histograms.

In addition to the overall achievable rate, the next section also compares the performance of half-marker and standard marker codes using more practical metrics, including bit error and symbol error rates.

Table I
OVERALL ACHIEVABLE RATE, R_a , WHEN $p_d = 0.05$ AND $p_s = 0.02$.

N_p	SMC1	HMC1	SMC2	HMC2
5	.48	.55	.43	.50
7	.52	.58	.54	.55
9	.53	.59	.55	.59
11	.51	.53	.56	.60
13	.48	.51	.56	.60
15	.46	.50	.55	.58

IV. NUMERICAL RESULTS

In this section, we provide numerical results to evaluate the performance of half-marker codes. We consider two half-marker codes, denoted by HMC1 and HMC2, corresponding to two standard marker codes, denoted by SMC1 and SMC2, as follows. SMC1 is an (N_p, \mathbf{m}_1) standard marker code with $\mathbf{m}_1 = (10)$, i.e., a code that inserts a marker symbol, 10, every N_p symbols. HMC1 is an (N_p, \mathbf{m}_1) half-marker code, i.e., two half-marker symbols are inserted every N_p symbols, and the inserted half-marker symbols are in the form $1x, 0x$. SMC2 is an (N_p, \mathbf{m}_2) standard marker code where two marker symbols, $\mathbf{m}_2 = (01, 10)$, are inserted every N_p symbols; and HMC2 is an (N_p, \mathbf{m}_2) half-marker code where four half-marker symbols are inserted every N_p symbols, and the inserted half-marker symbols are in the form $0x, 1x, 1x, 0x$.

Table I shows the overall achievable rate, R_a , defined in (8), for different marker coding schemes. In order to obtain an accurate estimate of R_a , we allow a large information sequence length of $n = 10^4$ bits. Note that by increasing N_p , the marker code rate, r_M , will increase, whereas $I(\mathbf{u}; \mathbf{L})$ will decrease. Due to this trade-off, there exists an optimal value of N_p for which $R_a = \frac{r_M}{n} \times I(\mathbf{u}; \mathbf{L})$ is maximized. As highlighted in Table I, the maximum overall achievable rate is .53, .59, .56, and .60, for SMC1, HMC1, SMC2, and HMC2, respectively. It is observed that the half-marker codes have the potential to increase the maximum achievable rates compared to their corresponding standard marker codes. For instance, the maximum achievable rate offered by HMC1 is 11% greater than that offered by SMC1. Also, we observe that for any given N_p , the value of R_a is larger for HMC1 (HMC2) compared to SMC1 (SMC2). Since for a given N_p , the rates of HMC1 and SMC1 are equal, we conclude that HMC1 achieves a larger mutual information, $I(\mathbf{u}; \mathbf{L})$, compared to SMC1. Similarly, for any given N_p , HMC2 achieves a larger mutual information compared to SMC2.

In Fig. 3, we simulate a concatenated LDPC-marker coding scheme, where a $(300, 150)$ LDPC code is employed as the outer code, i.e., vector \mathbf{u} of Fig. 1 is a codeword of this LDPC code. The employed LDPC code is regular and is constructed using Gallager's approach [19] with a variable node degree of 3 and a check node degree of 6. At the decoder side, the LLR vector, \mathbf{L} , generated by the FB decoder, is passed to an LDPC decoder which updates these LLRs and returns them as *a priori* information to the FB decoder. This exchange continues for a specified number of iterations, after which a hard decision, denoted as $\hat{\mathbf{u}}$, is made using the most up-to-

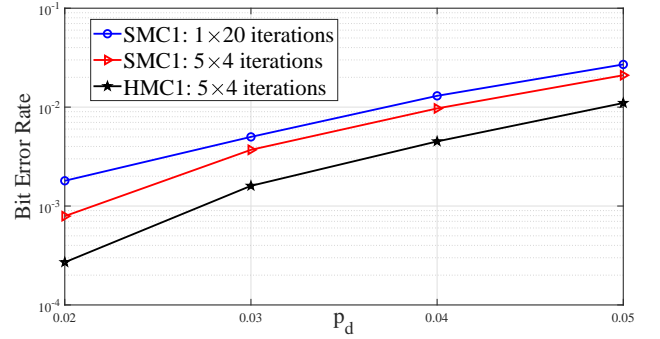


Figure 3. Bit error rates of concatenated LDPC-marker coding schemes, when $p_s = 0.02$ and $N_p = 6$.

date LLR values. We define the end-to-end bit error rate (BER) as $E \left[\frac{1}{n} \sum_{j=1}^n (u_j \oplus \hat{u}_j) \right]$, where $E[\cdot]$ and \oplus denote statistical expectation and exclusive-or (XOR) operation, respectively. We plot this BER when SMC1 or HMC1 is employed as the inner code. The label “5 × 4 iterations” in Fig. 3 indicates that each FB decoding step is followed by four LDPC decoding iterations, and the information is exchanged between the two decoders five times. It is observed that the scheme which employs HMC1 significantly outperforms the one which employs SMC1. Therefore, half-marker codes may significantly improve performance compared to standard marker codes, even at short block lengths, n . This observation is important since the state of the art DNA storage systems are only capable of synthesizing short-length DNA strands (due to the current synthesis technology limitations [1]). Also, a result labeled “1 × 20 iterations,” corresponding to an FB decoding step followed by 20 LDPC decoding iterations without exchanging information between the two decoders, is included in Fig. 3.

Figure 4 depicts the achievable rates for different marker patterns, determined via Monte Carlo simulation as described in detail in Section III. It is observed that the maximum achievable rate is larger in the case of half-marker codes. Specifically, the maximum achievable rates for SMC1 and SMC2 are 0.736 (achieved at $N_p = 13$) and 0.725 (achieved at $N_p = 17$), respectively; whereas the maximum achievable rates for HMC1 and HMC2 are 0.776 (achieved at $N_p = 13$) and 0.745 (achieved at $N_p = 17$), respectively. It is also observed that the half-marker code HMC1 outperforms the other codes in this setup for all values of $5 \leq N_p \leq 17$.

Figure 5 compares the symbol error rates (SER) of different coding schemes. To evaluate the SER, a hard decision on the symbol sequence is made after FB decoding, as follows:

$$\hat{s}_i = \underset{bb' \in \{00, \dots, 11\}}{\operatorname{argmax}} \rho_i^{bb'}, i \in \left\{ 1, \dots, \frac{n}{2} \right\} \quad (11)$$

The SER is then computed via Monte Carlo simulation of $E \left[\frac{2}{n} \sum_{i=1}^{n/2} \mathbf{1}_{s_i \neq \hat{s}_i} \right]$ where $\mathbf{1}_{s_i \neq \hat{s}_i}$ is an indicator function that returns 1 if $s_i \neq \hat{s}_i$ and 0 otherwise. The watermark code is implemented as described in [17], while the DNA-LM code follows [8], with its SER curve shown in ([8], Fig. 6-

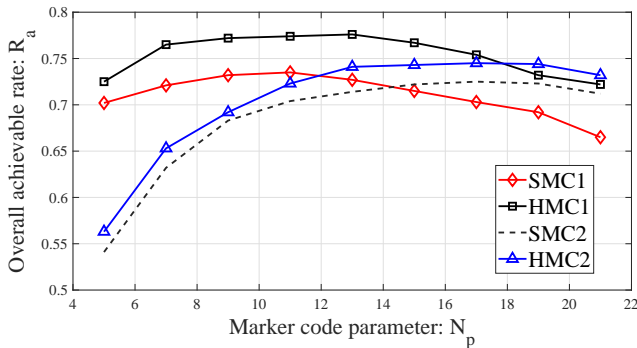


Figure 4. Overall achievable rate, for $p_d = 0.02$ and $p_s = 0.01$.

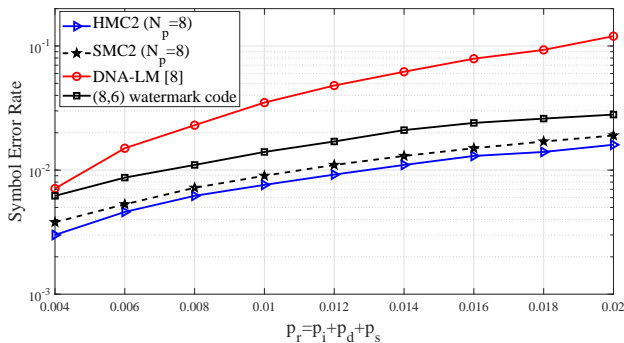


Figure 5. Comparison between the symbol error rates achieved by different synchronization codes.

a). The comparisons consider insertion errors using the IDS channel model from ([8], Fig. 2). Here, p_i denotes the insertion probability, and $p_r = p_i + p_d + p_s$ represents the mutation error rate [8], where we assume $p_s = 2p_i = 2p_d$ as in [8]. For the DNA-LM code, the original data sequence s consists of 180 symbols ([8], Table 4), and the encoded sequence x has 246 symbols. For SMC2 and HMC2, s also consists of 180 symbols, but it is encoded into x with 240 symbols by inserting either 2 standard marker symbols (for SMC2) or 4 half-marker symbols (for HMC2) every $N_p = 8$ symbols. For the watermark code, a binary sequence u of length 360 bits is encoded into $\frac{8}{6} \times 360 = 480$ bits using an (8, 6) watermark code. These 480 bits are then mapped to a symbol sequence x of length 240. Note that the DNA-LM code has a slightly longer block length; consequently, a slightly lower rate compared to the other codes.

As shown in Fig. 5, the marker codes outperform both the watermark and DNA-LM codes, with HMC2 achieving the lowest SER values among all schemes. However, we note that the DNA-LM code has lower decoding complexity compared to the other schemes [8].

V. CONCLUSIONS

We propose a new class of marker codes, referred to as half-marker codes, for DNA data storage systems. Although it cannot be guaranteed that half-marker codes will always outperform their corresponding standard marker codes, they provide us with

a larger class of marker codes to select from, and our extensive experiments show that they have the potential to improve the performance of various system setups and channel parameters, including the ones that are studied in this letter. Note that design of optimized concatenated LDPC–half-marker codes is also possible as a further extension.

REFERENCES

- [1] O. Milenkovic and C. Pan, “DNA-based data storage systems: A review of implementations and code constructions,” in *IEEE Transactions on Communications*, vol. 72, no. 7, pp. 3803–3828, July 2024.
- [2] I. Shomorony and R. Heckel, “DNA-based storage: Models and fundamental limits,” in *IEEE Transactions on Information Theory*, vol. 67, no. 6, pp. 3675–3689, June 2021.
- [3] D. Deamer, M. Akeson, and D. Branton, “Three decades of nanopore sequencing,” *Nature Biotechnol.*, vol. 34, no. 5, pp. 518–524, 2016.
- [4] W. Mao, S. N. Diggavi and S. Kannan, “Models and information-theoretic bounds for nanopore sequencing,” in *IEEE Transactions on Information Theory*, vol. 64, no. 4, pp. 3216–3236, April 2018.
- [5] D. Goshkoder, N. Polyanskiy and I. Vorobyev, “Codes correcting long duplication errors,” in *IEEE Transactions on Molecular, Biological, and Multi-Scale Communications*, vol. 10, no. 2, pp. 272–288, June 2024.
- [6] J. Luo, L. Mu, Y. Huang, Y. Yan, G. Han and Y. Zhong, “Two RRNS-based error correction schemes for DNA storage channels,” in *IEEE Communications Letters*, vol. 28, no. 12, pp. 2729–2733, Dec. 2024.
- [7] M. Kovačević and V. Y. F. Tan, “Asymptotically optimal codes correcting fixed-length duplication errors in DNA storage systems,” in *IEEE Communications Letters*, vol. 22, no. 11, pp. 2194–2197, Nov. 2018.
- [8] Z. Yan, C. Liang and H. Wu, “A segmented-edit error-correcting code with re-synchronization function for DNA-based storage systems,” in *IEEE Transactions on Emerging Topics in Computing*, vol. 11, no. 3, pp. 605–618, 1 July–Sept. 2023.
- [9] M. Welzel *et al.*, “DNA-Aeon provides flexible arithmetic coding for constraint adherence and error correction in DNA storage,” *Nature Commun.*, vol. 14, no. 1, pp. 1–10, 2023.
- [10] A. Banerjee, A. Lenz and A. Wachter-Zeh, “Sequential decoding of multiple sequences for synchronization errors,” in *IEEE Transactions on Communications*, vol. 72, no. 11, pp. 6660–6676, Nov. 2024.
- [11] T. Thanh Nguyen, K. Cai and P. H. Siegel, “A new version of q-ary Varshamov-Tenengolts codes with more efficient encoders: the differential VT codes and the differential shifted VT codes,” in *IEEE Transactions on Information Theory*, vol. 70, no. 10, pp. 6989–7004, Oct. 2024.
- [12] S. Wang, Y. Tang, J. Sima, R. Gabrys and F. Farnoud, “Non-binary codes for correcting a burst of at most t deletions,” in *IEEE Transactions on Information Theory*, vol. 70, no. 2, pp. 964–979, Feb. 2024.
- [13] F. F. Sellers Jr., “Bit loss and gain correction code,” *IRE Trans. Inf. Theory*, vol. 8, no. 1, pp. 35–38, Jan. 1962.
- [14] G. Ma, X. Jiao, J. Mu, H. Han and Y. Yang, “Deep learning-based detection for marker codes over insertion and deletion channels,” in *IEEE Transactions on Communications*, vol. 72, no. 10, pp. 5945–5959, Oct. 2024.
- [15] L. Welter, I. Maarouf, A. Lenz, A. Wachter-Zeh, E. Rosnes and A. G. I. Amat, “Index-based concatenated codes for the multi-draw DNA storage channel,” 2023 *IEEE Information Theory Workshop (ITW)*, Saint-Malo, France, 2023, pp. 383–388.
- [16] S. R. Srinivasavaradhan, S. Gopi, H. D. Pfister, and S. Yekhanin, “Trellis BMA: Coded trace reconstruction on IDS channels for DNA storage,” in *Proc. IEEE Int. Symp. Inf. Theory*, Melbourne, Australia, Jul. 2021.
- [17] M. C. Davey and D. J. Mackay, “Reliable communication over channels with insertions, deletions and substitutions,” *IEEE Trans. Inf. Theory*, vol. 47, no. 2, pp. 687–698, Feb. 2001.
- [18] F. Wang, D. Fertonani and T. M. Duman, “Symbol-level synchronization and LDPC code design for insertion/deletion channels,” in *IEEE Transactions on Communications*, vol. 59, no. 5, pp. 1287–1297, May 2011.
- [19] R. Gallager, “Low-density parity-check codes,” in *IRE Transactions on Information Theory*, vol. 8, no. 1, pp. 21–28, January 1962.
- [20] J. Haghghat, “Forward-backward decoding equations for a class of insertion deletion and substitution channels,” [Online]. Available: <https://github.com/Bilkent-CTAR-Lab>